A Modeled Hydrophobic Domain on the TCL1 Oncoprotein Mediates Association with AKT at the Cytoplasmic Membrane†

Samuel W. French,‡ Rhine R. Shen,‡ Patricia J. Koh,‡ Cindy S. Malone,§ Parag Mallick,|| and Michael A. Teitell*,‡,#,⊥

Department of Pathology and Laboratory Medicine, Microbiology and Immunology, UCLA-DOE Laboratory of Structural Biology and Molecular Medicine, Molecular Biology Institute and UCLA AIDS Institute, UCLA School of Medicine, Los Angeles, California 90095−1732

Received December 19, 2001; Revised Manuscript Received March 6, 2002

ABSTRACT: AKT has a critical role in relaying cell survival and proliferation signals initiated by ligand binding to surface receptors in mammalian cells. Induction of AKT serine/threonine kinase activity is augmented by the T-cell leukemia-1 (TCL1) oncoprotein through a physical association requiring the AKT pleckstrin homology domain. Here, we used molecular modeling and identified an exposed hydrophobic patch composed of two discontinuous amino acid stretches near one end of the TCL1 β-barrel that was required for a TCL1−AKT association. Site-directed mutations of this region did not affect TCL1 secondary structure, yet they disrupted interactions with AKT. This region was found in other members of the TCL1 oncoprotein family, such as TCL1b and MTCP1, and suggested a conserved, novel AKT binding domain. Interestingly, TCL1 and AKT co-localize in multiple cell compartments, but only extracts from the plasma membrane stimulate optimal complex formation in vitro. Identification of an AKT binding domain on TCL1 is an important step in deciphering the complex interactions that regulate AKT kinase activity in lymphocyte development and neoplasia within the immune system.

The T-cell leukemia-1 (*TCL1*)[1] oncogene was identified due to characteristic chromosomal translocations and inversions at 14q32.1 in clonal T-cell proliferations and malignancies (*1*). Repositioning of T-cell receptor α/δ or β-chain control sequences next to the *TCL1* coding region yields dysregulated T-cell specific expression. Evidence confirming a tumorigenic role for aberrant *TCL1* expression has been obtained from transgenic mouse studies that showed a slow progression to malignancy in overexpressing T-cells (*2*). The product of the *TCL1* gene is a 14-kDa protein that has been shown to localize in the cytoplasm and nucleus of expressing cells (*3*). Crystallographic studies indicated that TCL1 exhibits a novel β-barrel structural conformation (*4*). Studies of additional members of the TCL1 oncoprotein family, including TCL1b and MTCP1, showed that these proteins also adopt a similar β-barrel structural conformation (*5*−*8*). Recently, *TCL1* expression has been linked to specific stages of peripheral B-cell maturation and to specific classes of B-cell lymphoma (*9*−*12*). In lymph nodes, high-level TCL1 protein expression occurs in naïve mantle zone B-cells. This expression is progressively silenced as B-cells transit through reactive germinal centers and is extinguished during final development to nonproliferating memory or plasma cells (*9*, *13*). This pattern of TCL1 expression in B-cell development, coupled with its relatively weak oncogenic potential in human and transgenic mouse T-cells, caused us to postulate that TCL1 is involved mainly in cell survival and cell proliferation (*9*). Recent yeast-two-hybrid, co-immunoprecipitation and glutathione-*S*-transferase (GST) "pulldown" studies have shown that TCL1 binds and co-activates AKT (protein kinase-B or RAC-PK) supporting a role for TCL1 in cell survival and proliferation (*14*, *15*). Additional studies have also shown that TCL1 oligomerizes as dimers or trimers alone or bound to AKT in ill-defined in vitro and in vivo complexes (*14*, *16*).

AKT1, *AKT2*, and *AKT3* are mammalian homologues of *v-akt*, a viral oncogene isolated from the AKT8 virus that causes T-cell lymphomas in mice (*17*−*20*). Each *AKT* gene encodes an AKT isoform, designated AKT1, AKT2, and AKT3, respectively. AKT isoforms are roughly 60-kDa serine/threonine kinases that are differentially regulated and function in multiple signaling pathways (*21*). Activation of each AKT isoform is similar and is initiated by ligand binding to distinct membrane-bound receptor tyrosine kinases. In turn, this triggers distinct signaling cascades that begin with the activation of phosphatidylinositide-3′-OH kinase (PI3-K) and recruitment of AKT to the inner surface

† This work was supported by an Amgen/UC BioStar Award (S98-35 to M.A.T.), a UCLA CFAR Award (S.W.F. and M.A.T.), the Lymphoma Research Foundation of America (M.A.T.), a PHSNS Award (T32-CA09056 to C.S.M.), and the National Institutes of Health (GM40185 to P.M. and CA74929 to M.A.T.).

* To whom correspondence should be addressed: Department of Pathology and Laboratory Medicine, UCLA School of Medicine, MacDonald Research Laboratories, Room 4-760, 675 Charles E. Young Drive South, Los Angeles, CA 90095-1732. Telephone: 310-206-6754. Fax: 310-267-0382. E-mail: mteitell@ucla.edu.

‡ Department of Pathology and Laboratory Medicine.

§ Microbiology and Immunology.

|| UCLA-DOE Laboratory of Structural Biology and Molecular Medicine.

Molecular Biology Institute.

⊥ UCLA AIDS Institute.

[1] Abbreviations: TCL1, T-cell leukemia-1; GST, glutathione-*S*-transferase; PI3-K, phosphatidylinositide-3′-OH kinase; PH, pleckstrin homology; CD, circular dichroism; HA, hemaglutinin; MEF, murine embryonic fibroblast.

10.1021/bi016068o CCC: $22.00
Published on Web 04/17/2002

of the cytoplasmic membrane. This relocalization requires the pleckstrin homology (PH) domain of AKT, which directly binds to 3′-phosphorylated phosphoinositides. At the membrane, AKT is activated by a partially defined process involving lipid-mediated dimerization and phosphorylation of two critical residues, Thr308/309/305 and Ser473/474/472, on AKT1/2/3, respectively (*19*, *22*−*27*). The Thr308/309/305 residue is phosphorylated by phophoinositide dependent kinase 1 (PDK1), while the mechanism responsible for phosphorylation of Ser473/474/472 is not resolved (*28*). Activated AKT then increases cell survival through blockade of apoptotic signals mediated by BAD, caspase 9, I$\kappa\kappa$, Nur77, and the forkhead family of transcription factors (*21*, *29*, *30*).

An essential role for the PH domain of AKT isoforms has been shown for complex formation and increased activation by TCL1 family member proteins, yet the region(s) on TCL1 itself that contribute to this interaction are unknown (*14*, *15*, *31*). Although both TCL1 and AKT isoforms were reported to co-localize in the nucleus and cytoplasm, recruitment of AKT to the membrane during activation suggests that the cell membrane may be the actual site of TCL1/AKT complex formation. Furthermore, it has been reported that TCL1 augments or is required for AKT translocation into the nucleus (*15*). Yet, neither TCL1 nor AKT contain recognizable nuclear localization signals, suggesting that a TCL1/AKT complex may involve additional components that facilitate nuclear entry. Complicating this picture, stimulation of the B-cell antigen receptor appears to result in AKT phosphorylation with subsequent translocation of phosphorylated AKT into the nucleus by an unknown mechanism (*32*). Here, we performed molecular modeling analyses and identified a TCL1 interaction domain for AKT. We demonstrated the functional capacity of this domain with B-cell extracts using GST-fusion protein pulldown assays. Furthermore, we show that membrane, and possibly cytoskeletal, but not cytoplasmic or nuclear extracts, are required for optimal complex formation. These results yield a domain on TCL1, and a location within the cell, for therapeutic interventions designed to block inappropriate TCL1 activation of AKT in lymphoid malignancies.

MATERIALS AND METHODS

Structure Based Identification of a TCL1 Interaction Domain. Homologues of TCL1 were identified using the NCBI BLAST program and additional molecules containing structural similarity to TCL1 were identified within the FSSP database of Holm and Sander (*33*, *34*). These sequences created a set of TCL1 related sequences. We assembled a multiple alignment of these sequences guided by the alignments contained within the HSSP and FSSP databases. A TCL1 profile hidden Markov model, similar to those described by Karplus et al., was generated from the multiple alignment and used to identify additional, potential structural homologues of TCL1 (*35*). Newly identified sequences were then added to the model. An analysis of the emission probabilities of the final model revealed positions of unusual evolutionary conservation. Conserved positions were mapped to the 3-dimensional structure of TCL1. A simple patch analysis was performed to find sets of conserved residues that were clustered near each other on the 3D structure. Finally, clusters were analyzed for unusual surface characteristics, such as hydrophobicity.

GST−*TCL1 Fusion Protein Generation.* A human *TCL1* cDNA was PCR amplified with end-modified primers 5′-gaattcggatccGCCGAGTGCCCGACACTCGGGGAGGCA-3′ and 5′-cgggatcccgcaagcttgTACATCAGTCATCTGGCAG-CAGCTCG-3′ (lower case letters correspond to added restriction sites). The PCR product was cloned in-frame into the BamHI site of the pGEX-2T fusion protein vector (Amersham-Pharmacia, Piscataway, NJ) to create a *GST*−*TCL1* fusion gene. *GST*−*TCL1* construct integrity was verified by sequencing (data not shown). Primer pairs were synthesized for site-directed mutation of the TCL1 binding domain (QuikChange Kit, Stratagene, La Jolla, CA; primer sequences for mutants 1 through 6 are available upon request). Mutant construct integrity was confirmed by sequencing (data not shown). Once confirmed, wild-type and mutant GST-TCL1 fusion proteins were generated and purified on glutathione-sepharose 4B beads (Amersham-Pharmacia Biotech AB, Uppsala, Sweden) as previously described with subtle modifications (*36*). A control GST-E2c fusion protein was obtained as a kind gift from Dr. C. Denny (UCLA, Los Angeles, CA; *37*). Half of the bound beads were stored at −80 °C for pulldown experiments. The remaining beads were eluted five times with 500 μL of 50 mM Tris pH 8.0, 5 mM DTT, and 10 mM glutathione (Sigma, St. Louis, MO). Eluted fusion proteins were dialyzed two times against 1 mM sodium phosphate pH 7.2 and 20 mM sodium chloride. Isolated proteins were analyzed on 10% SDS−PAGE and were >95% pure (data not shown).

Circular Dichroism (CD). CD spectra were recorded using a Jasco J-715 instrument. Dialyzed wild-type and mutant GST-TCL1 fusion proteins were analyzed in a flat quartz cell with a path length of 0.1 cm. Spectra were obtained across a 195 to 260 nm wavelength range at 0.5 nm increments and represent an average of eight scans for each protein. Each recombinant protein spectrum was corrected by subtraction with a smoothed buffer spectrum. Corrected recombinant protein spectra were not smoothed. Protein concentrations were determined using the BCA assay (Pierce, Rockford, IL).

Tissue Culture. Cell lines were maintained at 37 °C in 5% CO_2 and grown in RPMI 1640 medium supplemented with 2 mM L-glutamine, 1 mM sodium pyruvate, 0.1 mM nonessential amino acids, 100 units/mL penicillin, 100 mg/mL streptomycin and 15% FBS. P3HR-1, BCBL-1, and Jurkat cell lines were provided as a kind gift from Dr. R. Sun (UCLA).

Whole Cell Extracts and Subcellular Fractionation. To prepare whole extracts, cells were washed twice with ice-cold 1× PBS, pH 7.2, lysed in NP-40 lysis buffer (50 mM Tris pH 7.6, 300 mM NaCl, 0.5% NP-40, 10% glycerol, 1 mM EDTA, and protease inhibitors), centrifuged at 15000*g* for 20 min at 4 °C and supernatants harvested. For fractionation studies, cells were collected by centrifugation, resuspended on ice in hypotonic lysis buffer E (10 mM Tris-HCl, pH 7.4, 10 mM KCl, 1.5 mM $MgCl_2$ with protease inhibitors), and disrupted with a dounce homogenizer. Ice cold homogenates were centrifuged at 16000*g* for 10 min at 4 °C. Supernatants were collected (cytosolic fraction). The pellets were washed five times each with 250 μL of buffer E and resuspended in 250 μL of buffer E plus 1% NP-40 detergent, incubated on ice for 15 min, and centrifuged at 16000*g* for 10 min at 4 °C. Supernatants were collected

(detergent soluble membrane fraction), and pellets again were washed two times with 250 μL of buffer E plus 1% NP-40 detergent. Pellets were resuspended in 250 μL of RIPA buffer (20 mM Tris, pH 8.0, 150 mM NaCl, 0.1% SDS, 1% NP-40, 0.5% deoxycholate, and 1 mM EDTA with protease inhibitors), sonicated for 2 s, and vortexed for 30 s. Lysates were centrifuged at 16000*g* for 30 min at 4 °C, and supernatants were collected (detergent insoluble cytoskeletal fraction). Pellets were resuspended in 20 mM Tris, pH 7.9, 1.5 mM $MgCl_2$, 0.2 mM EDTA, 420 mM KCl, and 1 mM DTT, incubated on ice for 30 min, centrifuged at 16000*g* for 15 min, and supernatants collected (nuclear fraction). Protein concentrations were determined using the Bradford assay (Bio-Rad, Hercules, CA).

Western Blot Analysis. A total of 8 μg of fractionated cell extract per lane were resolved in parallel 10 and 15% denaturing polyacrylamide gels followed by transfer to nitrocellulose membranes (Micron Separations Inc., Westborough MA). Western blotting was performed as previously described with the following modifications (*13*): One membrane was incubated with TCL1 antisera (1:7500), while a second membrane was incubated with phospho-AKT antibody (anti-Ser473; 1:2000; New England Biolabs, Beverly, MA). The filters were washed, incubated in HRP-linked anti-rabbit IgG (1:5000; New England Biolabs), washed, and exposed with ECL+Plus (Amersham-Pharmacia Biotech). The membranes were then stripped. In one set of experiments, one stripped membrane was reprobed with a Histone H1 antibody (1:1000; clone AE-4; Upstate Biotechnology, Lake Placid, NY) while the other stripped membrane was incubated with an AKT antibody (New England Biolabs). Both membranes were washed, incubated with anti-mouse-IgG-HRP (Promega, Madison, WI), and developed as before. In a separate experiment, a stripped membrane (without a cytoskeletal fraction) was incubated with B29 antisera (1:10000, a kind gift of Dr. Randolph Wall, UCLA), washed, incubated with a HRP-linked secondary reagent and developed as before.

GST-Fusion Protein Pulldown Assays. 10 μg of bead-linked wild-type or mutant GST-TCL1 fusion protein was incubated with 40 μg of whole cell extract in NP-40 lysis buffer for 1 h. The beads were pelleted, washed four times with lysis buffer, and separated by 10% SDS−PAGE. Western blots were performed with anti-AKT antibody (New England Biolabs) as described. Membranes were incubated with ponceau stain to confirm equal loading of GST-fusion proteins.

GST-fusion protein pulldown assays with ^{35}S-labeled HA-AKT were performed by in vitro transcription/translation of a hemaglutinin (HA)-tagged *AKT1* gene in a pBSIIKS+ DNA vector using the T7 TNT Quick Coupled Transcription/Translation system according to the manufacturer's instructions (Promega, Madison, WI). The expression construct was generated from a pCMV6-HA-AKT mammalian expression vector by standard cloning methods (*38*). GST-fusion protein pulldowns were performed by incubating 5 μL of ^{35}S-labeled HA-AKT with 10 μg of GST-fusion protein. A total of 20 μg of whole cell extract or subcellular fractionated extracts were added to specific tubes. Pulldowns were resolved on 10% SDS−PAGE, fixed in 40% methanol, and 10% acetic acid for 30 min and immersed in Amplify (Amersham-Pharmacia) for 30 min, dried, and exposed to film overnight. Coumassie blue staining demonstrated equal loading of wild-type and mutant GST-TCL1 fusion proteins used in each lane.

RESULTS

TCL1/AKT Complex Formation is Mediated by an Exposed Hydrophobic Domain on TCL1. The formation of a TCL1/AKT complex requires the PH domain of AKT (*15*, *31*). It is not known what part(s) of TCL1 is involved in this interaction. Studies by Lijnzaad and Argos have demonstrated a strong correlation between solvent-exposed surface patches of hydrophobic residues and protein interaction domains (*39*). Furthermore, regions of functional and structural importance are often evolutionarily conserved. Integrating these two observations, we searched for regions in TCL1 family member proteins that contain significant evolutionary conservation and surface-exposed hydrophobic residues. Computer generated models of human TCL1, TCL1b, MTCP1, and mouse TCL1 and MTCP1, based on published crystal and solution structures, yielded an evolutionarily conserved, exposed hydrophobic surface composed of two discontinuous amino acid segments, 15 to 21 and 72 to 80, in the TCL1 sequence. The region delimited by these amino acids forms a candidate interaction domain on TCL1 (Figure 1A and Table 1). Three separate, site-directed mutations of two to four residues were generated in each amino acid span, for a total of six TCL1 mutants, and GST-fusion protein expression constructs were created for pulldown experiments (Table 1).

Circular dichroism (CD) was performed to demonstrate that the site-directed mutations did not significantly alter the secondary structure of mutant GST-TCL1 fusion proteins from that of the wild-type protein. The CD spectra generated from wild-type and mutant GST-TCL1 fusion proteins showed minimal deviation from each other, indicating conservation of the overall secondary structure (Figure 1B and data not shown). The conformations of the major components of each fusion partner, including the α-helical component of GST and the β-pleated sheet component of TCL1, were maintained as demonstrated by comparable regions of the CD spectra between wild-type and mutant proteins. This was expected and reassuring for regional modifications of residues in TCL1 that are exposed on the surface and not part of the protein's internal hydrophobic core.

Incubation of wild-type GST-TCL1 fusion protein with BCBL1 (Figure 2A) and P3HR-1 B-cell or Jurkat T-cell (data not shown) extracts demonstrated the ability of TCL1 to form a complex with AKT in vitro. Control GST alone and a nonspecific GST-E2c fusion protein control showed minimal, nonspecific binding to AKT (Figure 2A and data not shown; *37*). Importantly, formation of this complex did not require the addition of exogenous TCL1 provided in the cell extracts since both BCBL-1 and Jurkat cells were TCL1-negative (*13*). Also, the presence of exogenous TCL1 did not interfere with or augment complex formation, since P3HR-1 cells contained relatively high levels of TCL1 (*1*, *13*). This observation was consistent with the formation of TCL1/AKT multimers between bead-bound GST-TCL1 and cellular AKT, with or without cellular TCL1, as previously described (*14*). Pulldown studies with extracts from BCBL-1 (Figure 2B), P3HR-1 or Jurkat cells (data not shown) using mutant

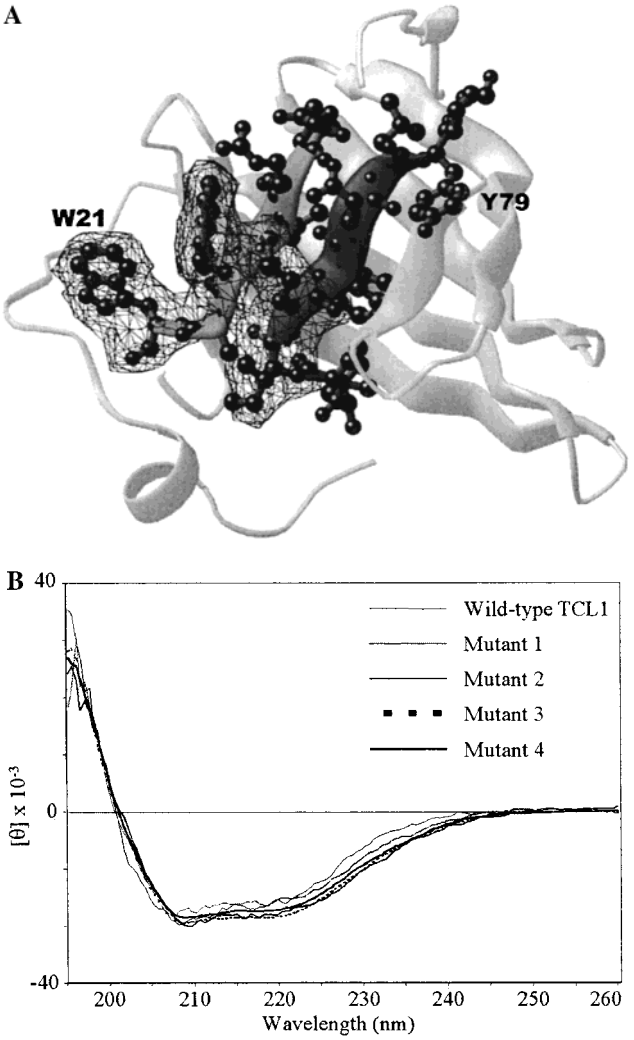

FIGURE 1: Structure of the identified TCL1 interaction domain and the effect of site-directed mutations on overall protein structure. (A) Ribbon diagram demonstrating the location of a conserved hydrophobic domain on one face of the TCL1 β-barrel near a flexible loop. Amino acids 15−21 are shaded medium-gray and 72−80 are colored dark gray. Residues W19, W21, I74, and I75 are depicted with van der Waals contours indicating a strip of the exposed hydrophobic patch. Labels are shown for W21 and Y79. Adapted from ref *4*. (B) Mutations of the conserved hydrophobic domain in TCL1 do not alter its secondary structure. Far-UV CD spectra of wild-type and mutant 1 through 6 GST-TCL1 fusion proteins (5 and 6 not shown for clarity) demonstrate nearly superimposable α-helical GST and β-pleated sheet TCL1 regions between wild-type and mutant fusion proteins.

GST−TCL1 fusion proteins showed a marked reduction in TCL1/AKT complex formation compared to results obtained with wild-type GST−TCL1. Furthermore, wild-type GST−TCL1 bound to in vitro synthesized and radiolabeled ^{35}S-HA-AKT more efficiently than any of the six mutant fusion proteins examined (Figure 2C). These data demonstrate that the interaction domain in TCL1 predicted from computer modeling studies has a role in mediating TCL1/AKT complex formation.

TCL1 and AKT are Concentrated in the Plasma Membrane and Cytoplasm of B-Cells. Immunofluorescent and confocal microscopy studies have demonstrated that wild-type TCL1 was localized within the cytoplasm and nucleus of transiently transfected murine embryonic fibroblast cells (MEF; *15*). AKT was seen only within the cytoplasm by microscopy in

Table 1: Identification of an Exposed Hydrophobic Domain in TCL1 Family Proteins and Site-Directed Mutants Used in this Study[a]

Family Member	Amino Acid Position															
	15	16	17	18	19	20	21	72	73	74	75	76	77	78	79	80
hTCL1	P	D	R	L*	W*	A*	W*	L	P	I	M	W*	Q*	L*	Y*	P
mTCL1	P	N	R	L	W	I	W	L	P	L	M	W	Q	L	Y	P
hMTCP1	P	D	H	L	W	V	H	L	P	L	M	W	Q	L	Y	P
mMTCP1	P	D	H	L	W	V	H	L	P	L	M	W	Q	L	Y	P
hTCL1b	P	G	R	L	W	I	Q	L	P	A	V	W	Q	L	Y	P
Consensus	P		RH	L	W			L	P		MV	W	Q	L	Y	P
Group	H		B	H	H	H		H	H	H	H	H	P	H	P	H
Mutant 1												R	R	R	H	
Mutant 2												G	E		D	
Mutant 3													L		F	
Mutant 4				R	R											
Mutant 5				R	R		R									
Mutant 6				Q	G	G	G									

[a] Sequence alignment between members of the TCL1 oncoprotein family reveals two conserved hydrophobic stretches of 7 and 9 amino acids. Positions 15−21 and 72−80 are listed for comparison between family members. Consensus positions are listed in the middle of the table along with their hydrophobic (H), basic (B), or polar (P) character. Residues exhibiting 100% conservation among all family members are highlighted in gray, and an asterisk indicates residues that are subjected to mutational analysis. At the bottom, mutations generated in the wild-type GST-TCL1 fusion protein are listed.

untransfected MEFs devoid of TCL1 or in MEFs transfected with a TCL1 molecule modified to localize exclusively within the nucleus. The interpretation of these data was that a TCL1/AKT complex must initially form within the cytoplasm prior to translocation of both molecules into the nucleus (*15*). However, MEFs and other normal or malignant nonlymphoid cell types do not express TCL1, leaving open the question of biological relevance for observations in these cells. Furthermore, the actual TCL1/AKT interaction site suggested by these results was extranuclear but not necessarily cytoplasmic.

Here, we determined the relative levels of TCL1 and AKT in the cytoplasm, membrane, cytoskeleton, and nuclear fractions of P3HR-1 and two other TCL1-expressing B-lymphocyte lines (BJAB and 2F7, data not shown). Assessments were made for equivalent total protein rather than for equivalent cell numbers per fraction, resulting in concentrations for TCL1 and AKT in each fraction. In addition to the cytoplasm, TCL1 was present at high concentration in the plasma membrane and low concentration in the cytoskeleton and nuclear fractions of all three TCL1-positive B-cell lines tested (Figure 3 and data not shown). For P3HR-1, the concentration of TCL1 in membrane extracts was roughly 7.5% of that seen in cytoplasmic extracts. Also, the concentration of both TCL1 and AKT in the nucleus was very low despite AKT activation as a result of cellular growth in 15% serum. By far, the highest concentration of Ser-473 phosphorylated, activated AKT was found in the membrane (Figure 3). Since TCL1 augments AKT activation through binding and oligomerization, the co-localization of high concentration TCL1 and activated AKT at the membrane suggests that this is the site of TCL1/AKT complex formation. Blotting for histone H1, a nuclear marker, and for Igβ (CD79b), a cell-surface marker of the B-cell antigen receptor, indicated that this isolation scheme yielded highly enriched subcellular fractions with little cross-contamination in all B-cell lines examined. Our data show that TCL1 concentra-

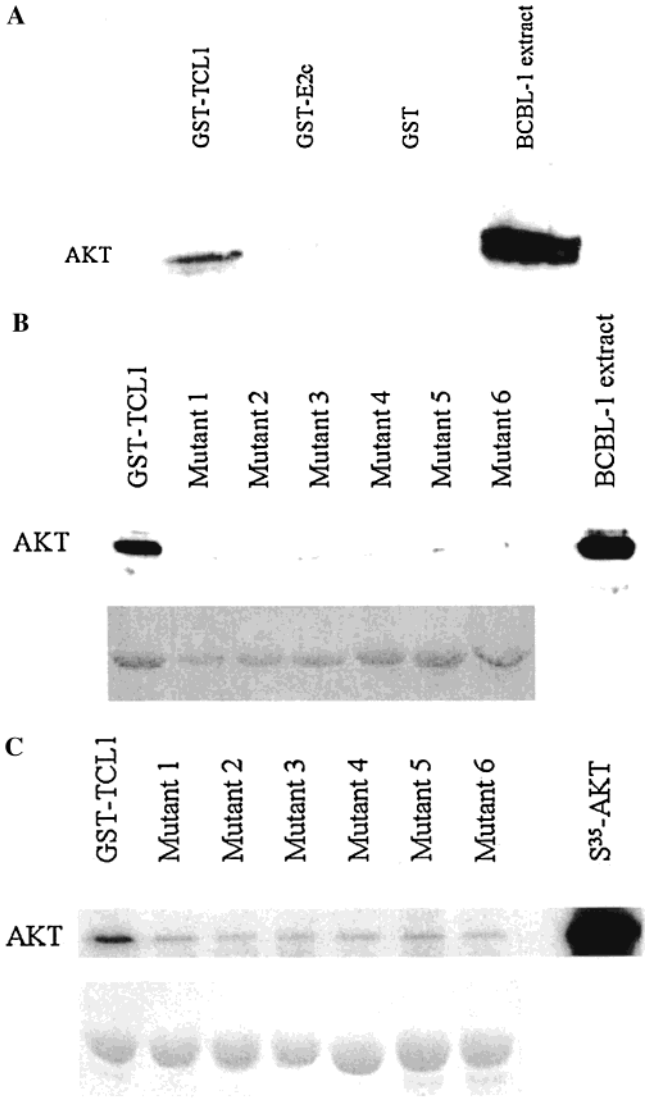

FIGURE 2: Pulldown assays demonstrate that wild-type GST-TCL1, in contrast to site-directed mutants 1 through 6, form a complex with AKT. (A) Pulldown assays were performed with BCBL-1 whole B-cell extracts followed by western analysis for AKT. Wild-type TCL1 binds AKT more effectively than control fusion protein GST-E2c or GST alone. (B) Pulldowns demonstrate that amino acid substitutions in the identified TCL1 interaction domain interfere with AKT complex formation. Wild-type and mutant 1 through 6 GST-TCL1 fusion proteins are shown interacting with BCBL-1 B-cell extracts. Ponceau staining of the western blot membrane shows equal amounts of fusion protein used in each lane examined in the panel at the bottom of the figure. Equivalent BCBL-1 extract was used in each lane. (C) Pulldown assay with GST-TCL1 wild-type and mutant 1 through 6 fusion proteins using in vitro transcribed and translated S^{35}-radiolabeled AKT. Mutant GST-TCL1 fusion proteins show decreased complex formation compared to wild-type GST-TCL1 with in vitro manufactured AKT. Coumassie blue staining demonstrates equal loading of the fusion proteins in the panel at the bottom of the figure.

tions in three TCL1-positive B-cell lines were highest in the cytoplasm followed by the plasma membrane, where TCL1 could interact with AKT or AKT-associated proteins or lipids. In addition, low concentrations of TCL1 and activated AKT in the nucleus of these three B-cell lines were observed despite the evident activation of AKT at the plasma membrane (Figure 3 and data not shown).

TCL1 is Inefficient at Forming a Complex with In Vitro Translated AKT. Prior studies suggesting that a cytoplasmic

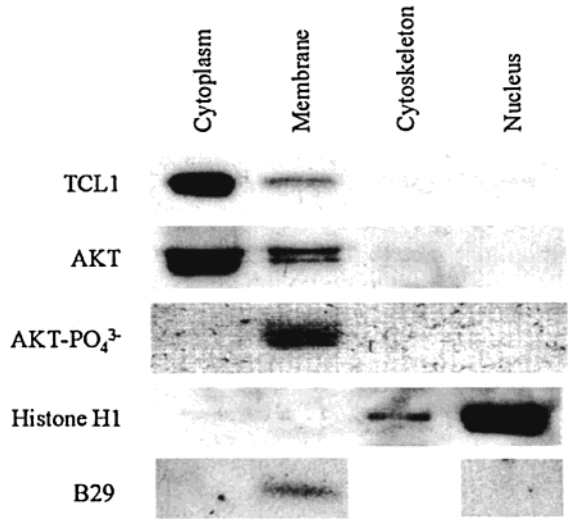

FIGURE 3: Distinct TCL1 and AKT protein concentrations within subcompartments of P3HR-1 B-cells. Each lane contains 8 μg of total protein isolated from the indicated cellular location. Western analysis demonstrates high TCL1 and AKT concentrations in the cytoplasm and plasma membrane (top two panels). Low TCL1 and AKT protein densities occur in the cytoskeleton and nucleus. AKT with ser-473 phosphorylation localizes to the membrane fraction (third panel). Histone H1 and Igβ controls for effectiveness of subcellular fractionation is shown (bottom two panels).

interaction between TCL1 and AKT facilitates nuclear entry are confounded by the lack of recognizable nuclear localization signals in either TCL1 or AKT protein sequences. Although we did not detect abundant TCL1 or AKT in the nucleus of three activated B-cell lines, the identification of additional components in a TCL1/AKT complex could prove critical for even small amounts of nuclear relocalization barely at our level of detection. Previous studies have shown that TCL1 and AKT co-immunoprecipitate in extracts from cells expressing high levels of TCL1 (*14*, *15*). These studies did not address whether these two molecules are precipitated alone or as part of a larger, heterogeneous complex. To determine whether the interaction between TCL1 and AKT is augmented by or requires another component, GST-TCL1 fusion protein pulldowns were performed with in vitro transcribed/translated, ^{35}S-radiolabeled HA-AKT. In this assay, GST-TCL1 interacted poorly with radiolabeled AKT, while GST-TCL1 bound a markedly increased fraction of ^{35}S-HA-AKT when TCL1-negative BCBL-1 cell extracts were also present (Figure 4A). However, control pulldowns with GST-TCL1 mutants were not rescued by the addition of extract and did not efficiently bind ^{35}S-HA-AKT, as expected, if this exposed hydrophobic domain was required for complex formation (Figure 4A and data not shown). These results indicated that cell extracts supply additional element(s) required for efficient complex formation between TCL1 and AKT. Moreover, the interaction between TCL1 and AKT did not require the activation of AKT since in vitro translated AKT is unphosphorylated, consistent with the identification of a TCL1/AKT complex in the yeast-two-hybrid system (*14*).

The Plasma Membrane, not the Cytoplasm or Nucleus, Provides a Complex Enhancing Factor. Since TCL1 and AKT co-localized at high concentration in the membrane and cytoplasm of B-cells (Figure 3), factors enhancing their interaction could be present in one or both of these locations.

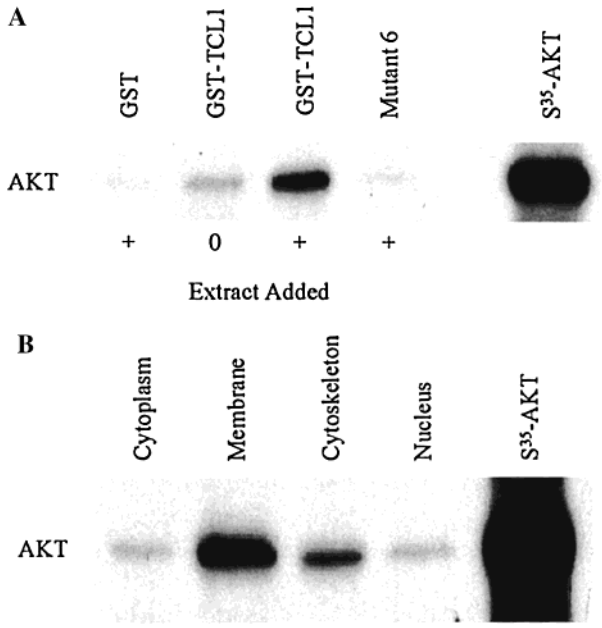

FIGURE 4: Pulldown assays performed with in vitro translated, radiolabeled AKT demonstrate that an element located primarily in the plasma membrane is required for efficient TCL1/AKT complex formation. (A) Control GST and control GST-TCL1 mutant 6 do not form a complex with AKT above background while wild-type GST-TCL1 with total cell extracts added markedly increases binding of input AKT. Inefficient, low-level ^{35}S-AKT binding to GST-TCL1 fusion proteins was reproducibly seen and appears similar to results recently reported for GST-TCL1 interactions with AKT3 (*31*). (B) Pulldown of in vitro synthesized AKT reconstituted with different subcellular fractions show that factors required for efficient complex formation are primarily located in the plasma membrane and minimally present in the cytoskeleton. Reconstitution with either cytoplasmic or nuclear fractions does not augment complex formation above the low-level binding seen without added extracts.

GST-TCL1 pulldown assays with S^{35}-HA-AKT were performed with extracts added from subcellular fractionation of TCL1-negative BCBL-1 cells (Figure 4B). Fractions from the membrane and to some extent from the cytoskeleton, but surprisingly not from the cytoplasm or nucleus, strongly enhanced the interaction between TCL1 and AKT. These results support a model in which a TCL1/AKT complex forms during AKT activation and is associated with the membrane recruitment phase of AKT after a signal is delivered through PI3-K activation. The moderate increase in interaction seen with the addition of cytoskeletal components suggests that an enhancing factor is also present in this location. Of note, enhancing factors were not TCL1, which was negative in BCBL-1 cells, or AKT, which was present at high concentrations in nonenhancing cytoplasmic extracts.

DISCUSSION

We used molecular modeling to define a functional region on the TCL1 oncoprotein that was required for efficient intermolecular interactions with AKT. This region is comprised of an exposed hydrophobic surface of two discontinuous β-pleated sheets containing residues 15 to 21 and 72 to 80. Our data do not address a previously proposed but untested region for intermolecular interactions on the opposite face of TCL1 family molecules, such as MTCP1, suggested by Yang et al. (*5*). Instead, we have characterized an additional interaction surface. Alterations in either amino acid stretch strongly reduced the ability of TCL1 to form a complex with AKT, while the overall conformation of the protein was maintained. The very slight broadening observed in both the α-helical and β-sheet regions of the CD spectra are within the error tolerance for this technique. As such, our study represents an early demonstration of a functional interacting domain for a TCL1 family member protein. These results were found with both pulldowns on whole cell extracts and in pulldowns with in vitro transcribed/translated AKT with fractionated extracts added back.

Given its interactions with AKT, the presence of TCL1 in the cytoplasmic membrane fraction is intriguing. This interaction depends on the PH domain of AKT, which is also required for attachment to 3′-phosphorylated phosphoinositides on the inner surface of the cell membrane during activation. Our results indicate that TCL1/AKT complex formation also occurs at this site. The observation that anchoring AKT to the cytoplasmic membrane by myristylation caused overexpressed TCL1 in MEF cell nuclei to relocate into the cytoplasm also lends support to our observation that the membrane is the physiologically relevant site for a TCL1/AKT interaction (*15*). Also, we have evidence for additional components in the cytoplasmic membrane fraction that augments this interaction. It will be important to determine the identity of these elements and the mechanism(s) of their action. One possibility is that 3′-phosphorylated phosphoinositides could augment the TCL1/AKT interaction. Recent studies have shown that 3′-phosphorylated phosphoinositides and the enzymes that process them are present in the membrane, cytoskeleton and nuclear subcompartments of mammalian cells (reviewed in ref *40*). The simple addition of these phospholipids is therefore unlikely to account for the increased binding affinity with membrane and cytoskeleton fractions observed, given the lack of augmented binding between TCL1 and AKT upon addition of nuclear extracts.

The very low concentrations of TCL1 and AKT in the nucleus of B-cells, determined by Western analysis, differs from results obtained by immunofluorescence and confocal microscopy studies on TCL1-transfected MEF cells (*15*). This difference can be accounted for by several possibilities. Transient transfection of MEF cells results in markedly exaggerated levels of TCL1 and HA-AKT, possibly causing nonspecific spillover into other cellular compartments. Also, MEF cells are an inappropriate cell type for TCL1 trafficking studies since TCL1 is not expressed in these cells and unknown companion molecules may impact normal routing. In contrast, the localization and binding studies presented here used B-cells in which TCL1 is normally expressed and therefore represents a more accurate physiologic approximation.

Identification of a new, conserved interaction domain on TCL1 has important implications for the function of TCL1 family proteins in development, signaling and neoplasia. TCL1 is not expressed in all cell types or at all stages of development, although signals are continuously transmitted from ligand−receptor interactions through AKT activation in mammalian cells. Therefore, other proteins, including additional members of the TCL1 oncoprotein family, may also mediate co-activation of AKT. In fact, evidence for a physical interaction and AKT activation between TCL1b or

MTCP1 and specific AKT isoforms has recently been obtained (*14*, *31*). Disruption of the identified interaction domain, by creation of dominant negative TCL1 proteins, could attenuate signals delivered through AKT and possibly reroute AKT trafficking in cells. Development of such reagents could have therapeutic benefit for the numerous diseases with abnormally strong or sustained AKT signaling, largely due to defects in the upstream tumor suppressor PTEN or due to dysregulated expression of TCL1 family member oncoproteins. Although we have identified an important AKT binding domain on TCL1, a systematic evaluation of the specific residues that mediate a TCL1/AKT interaction, along with identification of additional complex components, is required to develop potentially exciting therapeutic agents.

ACKNOWLEDGMENT

We thank Dr. Martin Phillips and Jennifer Lee for technical assistance and Dr. Masayuki Noguchi for technical advice. We are indebted to Dr. Randolph Wall, Dr. Peter Edwards, Dr. Richard Gatti, and members of the Teitell and Wall laboratories for helpful discussions and critical readings of the manuscript.

Note Added in Proof: During review of this manuscript, an independent study was published identifying key residues in an interaction domain between TCL1 and AKT [Kunstle, G., Laine, J., Pierron, G., Kagami, S. S., Nakajima, H., Hoh, F., Roumestand, C., Stern, M. H., and Noguchi, M. (2002) *Mol. Cell. Biol. 22*, 1513−25).

REFERENCES

1. Virgilio, L., Narducci, M. G., Isobe, M., Billips, L. G., Cooper, M. D., Croce, C. M., and Russo, G. (1994) *Proc. Natl. Acad. Sci. U.S.A. 91*, 12530−4.
2. Virgilio, L., Lazzeri, C., Bichi, R., Nibu, K., Narducci, M. G., Russo, G., Rothstein, J. L., and Croce, C. M. (1998) *Proc. Natl. Acad. Sci. U.S.A. 95*, 3885−9.
3. Fu, T. B., Virgilio, L., Narducci, M. G., Facchiano, A., Russo, G., and Croce, C. M. (1994) *Cancer Res. 54*, 6297−301.
4. Hoh, F., Yang, Y. S., Guignard, L., Padilla, A., Stern, M. H., Lhoste, J. M., and van Tilbeurgh, H. (1998) *Structure 6*, 147−55.
5. Yang, Y. S., Guignard, L., Padilla, A., Hoh, F., Strub, M. P., Stern, M. H., Lhoste, J. M., and Roumestand, C. (1998) *J. Biomol. NMR 11*, 337−54.
6. Fu, Z. Q., Du Bois, G. C., Song, S. P., Kulikovskaya, I., Virgilio, L., Rothstein, J. L., Croce, C. M., Weber, I. T., and Harrison, R. W. (1998) *Proc. Natl. Acad. Sci. U.S.A. 95*, 3413−8.
7. Guignard, L., Padilla, A., Mispelter, J., Yang, Y. S., Stern, M. H., Lhoste, J. M., and Roumestand, C. (2000) *J. Biomol. NMR 17*, 215−30.
8. Hallas, C., Pekarsky, Y., Itoyama, T., Varnum, J., Bichi, R., Rothstein, J. L., and Croce, C. M. (1999) *Proc. Natl. Acad. Sci. U.S.A. 96*, 14418−23.
9. Teitell, M., Damore, M. A., Sulur, G. G., Turner, D. E., Stern, M. H., Said, J. W., Denny, C. T., and Wall, R. (1999) *Proc. Natl. Acad. Sci. U.S.A. 96*, 9809−14.
10. Teitell, M. A., Thompson, A. D., Sorensen, P. H., Shimada, H., Triche, T. J., and Denny, C. T. (1999) *Lab. Invest. 79*, 1535−43.
11. Nakayama, I., Murao, S., Kitazawa, S., Azumi, A., Yamamoto, M., and Maeda, S. (2000) *Pathol. Int. 50*, 191−199.
12. Narducci, M. G., Pescarmona, E., Lazzeri, C., Signoretti, S., Lavinia, A. M., Remotti, D., Scala, E., Baroni, C. D., Stoppacciaro, A., Croce, C. M., and Russo, G. (2000) *Cancer Res. 60*, 2095−100.
13. Said, J. W., Hoyer, K. K., French, S. W., Rosenfelt, L., Garcia-Lloret, M., Koh, P. J., Cheng, T. C., Sulur, G. G., Pinkus, G. S., Kuehl, W. M., Rawlings, D. J., Wall, R., and Teitell, M. A. (2001) *Lab. Invest. 81*, 555−64.
14. Laine, J., Kunstle, G., Obata, T., Sha, M., and Noguchi, M. (2000) *Mol. Cell. 6*, 395−407.
15. Pekarsky, Y., Koval, A., Hallas, C., Bichi, R., Tresini, M., Malstrom, S., Russo, G., Tsichlis, P., and Croce, C. M. (2000) *Proc. Natl. Acad. Sci. U.S.A.*
16. Du Bois, G. C., Song, S. P., Kulikovskaya, I., Virgilio, L., Varnum, J., Germann, M. W., and Croce, C. M. (1998) *Protein Expr. Purif. 12*, 215−25.
17. Staal, S. P., Hartley, J. W., and Rowe, W. P. (1977) *Proc. Natl. Acad. Sci. U.S.A. 74*, 3065−7.
18. Staal, S. P. (1987) *Proc. Natl. Acad. Sci. U.S.A. 84*, 5034−7.
19. Bellacosa, A., Testa, J. R., Staal, S. P., and Tsichlis, P. N. (1991) *Science 254*, 274−7.
20. Bellacosa, A., Franke, T. F., Gonzalez-Portal, M. E., Datta, K., Taguchi, T., Gardner, J., Cheng, J. Q., Testa, J. R., and Tsichlis, P. N. (1993) *Oncogene 8*, 745−54.
21. Datta, S. R., Brunet, A., and Greenberg, M. E. (1999) *Genes Dev. 13*, 2905−27.
22. Coffer, P. J., and Woodgett, J. R. (1991) *Eur. J. Biochem. 201*, 475−81.
23. Burgering, B. M., and Coffer, P. J. (1995) *Nature 376*, 599−602.
24. Andjelkovic, M., Jakubowicz, T., Cron, P., Ming, X. F., Han, J. W., and Hemmings, B. A. (1996) *Proc. Natl. Acad. Sci. U.S.A. 93*, 5699−704.
25. Kohn, A. D., Takeuchi, F., and Roth, R. A. (1996) *J. Biol. Chem. 271*, 21920−6.
26. Franke, T. F., Kaplan, D. R., Cantley, L. C., and Toker, A. (1997) *Science 275*, 665−8.
27. Soskic, V., Gorlach, M., Poznanovic, S., Boehmer, F. D., and Godovac-Zimmermann, J. (1999) *Biochemistry 38*, 1757−64.
28. Chan, T. O., Rittenhouse, S. E., and Tsichlis, P. N. (1999) *Annu. Rev. Biochem. 68*, 965−1014.
29. Brunet, A., Bonni, A., Zigmond, M. J., Lin, M. Z., Juo, P., Hu, L. S., Anderson, M. J., Arden, K. C., Blenis, J., and Greenberg, M. E. (1999) *Cell 96*, 857−68.
30. Pekarsky, Y., Hallas, C., Palamarchuk, A., Koval, A., Bullrich, F., Hirata, Y., Bichi, R., Letofsky, J., and Croce, C. M. (2001) *Proc. Natl. Acad. Sci. U.S.A. 98*, 3690−4.
31. Laine, J., Kunstle, G., Obata, T., and Noguchi, M. (2001) *J. Biol. Chem. 13*, 3743−51.
32. Astoul, E., Watton, S., and Cantrell, D. (1999) *J. Cell. Biol. 145*, 1511−20.
33. Altschul, S. F., Madden, T. L., Schaffer, A. A., Zhang, J., Zhang, Z., Miller, W., and Lipman, D. J. (1997) *Nucleic Acids Res. 25*, 3389−402.
34. Holm, L., and Sander, C. (1996) *Nucleic Acids Res. 24*, 206−9.
35. Karplus, K., Barrett, C., and Hughey, R. (1998) *Bioinformatics 14*, 846−56.
36. Frangioni, J. V., and Neel, B. G. (1993) *Anal. Biochem. 210*, 179−87.
37. Arvand, A., Bastians, H., Welford, S. M., Thompson, A. D., Ruderman, J. V., and Denny, C. T. (1998) *Oncogene 17*, 2039−45.
38. Datta, K., Franke, T. F., Chan, T. O., Makris, A., Yang, S. I., Kaplan, D. R., Morrison, D. K., Golemis, E. A., and Tsichlis, P. N. (1995) *Mol. Cell. Biol. 15*, 2304−10.
39. Lijnzaad, P., and Argos, P. (1997) *Proteins 28*, 333−43.
40. Maraldi, N. M., Zini, N., Santi, S., and Manzoli, F. A. (1999) *J. Cell. Physiol. 181*, 203−17.

BI016068O